Three-Dimensional Ultrastructural Analysis of the *Saccharomyces cerevisiae* Mitotic Spindle

Mark Winey, Cynthia L. Mamay, Eileen T. O'Toole,* David N. Mastronarde,* Thomas H. Giddings, Jr., Kent L. McDonald,* and J. Richard McIntosh*

Department of Molecular, Cellular and Developmental Biology, and *Boulder Laboratory for 3D Fine Structure, University of Colorado–Boulder, Boulder, Colorado 80309-0347

Abstract. The three dimensional organization of microtubules in mitotic spindles of the yeast *Saccharomyces cerevisiae* has been determined by computer-aided reconstruction from electron micrographs of serially cross-sectioned spindles. Fifteen spindles ranging in length from 0.6–9.4 μm have been analyzed. Ordered microtubule packing is absent in spindles up to 0.8 μm, but the total number of microtubules is sufficient to allow one microtubule per kinetochore with a few additional microtubules that may form an interpolar spindle. An obvious bundle of about eight interpolar microtubules was found in spindles 1.3–1.6 μm long, and we suggest that the ~32 remaining microtubules act as kinetochore fibers. The relative lengths of the microtubules in these spindles suggest that they may be in an early stage of anaphase, even though these spindles are all situated in the mother cell, not in the isthmus between mother and bud. None of the reconstructed spindles exhibited the uniform populations of kinetochore microtubules characteristic of metaphase. Long spindles (2.7–9.4 μm), presumably in anaphase B, contained short remnants of a few presumed kinetochore microtubules clustered near the poles and a few long microtubules extending from each pole toward the spindle midplane, where they interdigitated with their counterparts from the other pole. Interpretation of these reconstructed spindles offers some insights into the mechanisms of mitosis in this yeast.

THE structure of the mitotic spindle and its function have been studied in a wide variety of organisms, yielding a few global observations about spindle structure. In general, spindles are organized from two spindle poles, each of which nucleates several classes of microtubules. These classes include astral, kinetochore, and interpolar spindle microtubules. The astral microtubules are not part of the spindle per se, but can be involved in the orientation, and perhaps the elongation of the spindle. Kinetochore microtubules connect the chromosomes to the spindle poles and are involved in chromosome movements. The interpolar spindle microtubules extend from each spindle pole, interdigitate with their counterparts from the other pole, and are involved in separating the poles with their attached chromosomes during anaphase B. This generic view of spindle organization is thought by many to hold true for most spindles, including that of the budding yeast, *Saccharomyces cerevisiae.* However, in spite of extensive studies of mitosis in this organism by molecular and genetic techniques, little information is available concerning the organization of its mitotic spindle.

The budding yeast cell cycle does not include cytologically discernable chromosome condensation or nuclear envelope breakdown. The stages of mitosis therefore can be difficult to determine, especially when the available information is based on visualization of spindle morphology by immunofluorescence or by EM of longitudinal sections. To understand chromosome movements, mutations that lead to defects in mitosis have been identified in a large number of yeast genes. Our understanding of the roles played by these genes in spindle function is based, in part, on the comparison of mutant phenotypes with the structure observed in wild-type cells. When structure is determined by immunofluorescent staining of microtubules, comparisons are made to the study of wild-type cells by Kilmartin and Adams (1984). The work of Byers and Goetsch (for review see Byers, 1981*a*) and Peterson and Ris (1976) has similarly served as the benchmark of wild-type spindle structure as viewed in the electron microscope. Wild-type spindle structures throughout the cell cycle have been described by Byers and Goetsch (1974, 1975*a*). This analysis included the characterization of wild-

Please address all correspondence to M. Winey, Department of Molecular, Cellular, and Developmental Biology, University of Colorado, Boulder, CO 80309-0347. Tel.: (303) 492-3409. Fax: (303) 492-7744.

The current address of C. L. Mamay is Molecular Toxicology and Environmental Health Sciences Program, School of Pharmacology, University of Colorado Health Sciences Center, Denver, CO 80231.

The current address of K. L. McDonald is Electron Microscope Laboratory, 26 Giannini Hall, University of California, Berkeley, CA 94720.

type spindles, and those found at various cell division cycle (*cdc*) mutant arrests, and has provided key data for the interpretation of cell cycle stages in yeast.

Understanding the mitotic mechanism in *S. cerevisiae*, defining discrete segments of the cell cycle, and interpreting mutant phenotypes would all benefit from high resolution studies of microtubule organization. Our current understanding of the distribution of spindle microtubules comes primarily from the work of Peterson and Ris (1976) and King et al. (1982). Peterson and Ris (1976) used serial semi-thick (0.25 μm) to thick (1 μm) sections and negatively stained whole mounts to analyze the three-dimensional distribution of spindle microtubules. They concluded that yeast has a conventional metaphase, followed by the shortening of kinetochore microtubules (anaphase A) of which they found an average of 14 microtubules for haploid strains. Continuous (pole-to-pole) microtubules were estimated to number about seven in haploid strains and this number was assumed to remain constant throughout spindle elongation. They found no evidence for overlapping microtubules and thus no support for a mechanism of spindle elongation involving microtubule sliding. King et al. (1982) used negatively stained images of isolated spindle whole mounts to reach similar conclusions. Up to 10 pole-to-pole microtubules were found in early spindles (1 μm length), but after the spindles elongated to ~4 μm, only one continuous microtubule was seen between the two spindle pole bodies. The obvious conclusion from these data was that spindle elongation took place by microtubule growth, not microtubule sliding.

Three-dimensional (3D)[1] reconstruction of organelles or cells from electron micrographs of serial sections has proven to be an important tool in understanding biological mechanisms. Indeed, Peterson and Ris (1976) did report some success in reconstructing spindles from serial cross-sections for the purpose of counting microtubules, as did Byers (1981*b*) in the analysis of the monopolar spindles found at the *cdc31* arrest. Similar reconstructions of synaptonemal complexes from meiotic yeast cells (Byers and Goetsch, 1975*b*) yielded an approximate number of chromosomes for this organism. More recently, computer-aided reconstruction of entire yeast cells has been accomplished (Baba et al., 1989). Computer programs have been developed that are specifically designed to reconstruct microtubule systems from serial cross sections (McDonald et al., 1991). These tools have been used to analyze spindle structure in mammalian tissue culture cells (McDonald et al., 1992; Mastronarde et al., 1993) and in *Schizosaccharomyces pombe* (Ding et al., 1993). In this paper, we have used improved fixation protocols and computer-assisted 3D reconstruction to analyze spindle structure in *S. cerevisiae*. We present data from 15 spindles ranging in length from 0.63 μm to 9.41 μm. Our results differ from the previous reports by Peterson and Ris (1976) and King et al. (1982). The spindle reconstructions presented here have many conventional attributes and some that are unconventional.

1. *Abbreviations used in this paper*: 3D, three-dimensional; FS, freeze substitution; HPF, high pressure freezing; NDA, neighbor density analysis; SPB, spindle pole body.

Materials and Methods

Strains and Cell Culture

The yeast strains used were S288c (genotype: α, *gal2*; source: R. K. Mortimer) and the S288c-background diploid D8Bx5Ca (genotype: a/α, *his3Δ200/his3Δ200*, *leu2-3,112/leu2-3,112*, *trp1Δ1/trp1Δ1*, *ura3-52/ura3-52*; source: this study). Yeast cells were grown in YEPD (Sherman, 1981) at 30°C in a shaking water bath. Cells were harvested in mid-log phase at a density of 1–5 × 10^6 cells/ml.

Preparation of Cells for Electron Microscopy

For high pressure freezing (HPF), aliquots (7–10 ml) of cells were withdrawn from log phase cultures and harvested by vacuum filtration on a 0.45-μm filter (Millipore Corp., Bedford, MA). A slight residue of growth medium was left on the filter to prevent drying. The cell paste was transferred to sample holders (Dahl and Staehelin, 1989) and the samples were frozen in a Balzers HPM010 high pressure freezer (Bal-Tec Corp., Middlebury, CT) and then stored under liquid nitrogen until freeze-substitution. Each sample was frozen within 2 min of removal from the culture flasks in a shaker bath and within 30–45 s of being captured on the filter.

HPF fixed cells were processed using a modified method of Ding et al. (1991). Briefly, the cells were freeze-substituted in 0.1% tannic acid in acetone at −90°C for 5 d and then fixed in 2% osmium tetroxide in acetone at −20°C for 1 d and at 4°C overnight. Fixed samples were rinsed in acetone, warmed to room temperature, removed from the specimen holders and embedded in Spurrs resin. For conventional fixation, glutaraldehyde fixed yeast cells were prepared and embedded in Spurrs resin as described by Byers and Goetsch (1991). Serial thin sections (30–50 nm) were cut on a Reichert Ultracut E Microtome (Leica Instruments, Wien, Austria). Sections were placed on 1 × 2 mm Formvar-coated slot grids, and poststained with 2% uranyl acetate in 70% methanol for 4 min and aqueous lead citrate for 2 min.

Microscopy

Sections were viewed in a CM10 electron microscope (Philips Electronic Instruments Co., Mahwah, NJ) equipped with a rotating grid holder and a ±60° goniometer stage operating at 80 kV. When cells containing spindle microtubules in approximate cross-section were detected, the goniometer stage controls were used to rotate and tilt the grid to maximize the circular cross section profiles of microtubules. For those data sets where tilts were adjusted while collecting the images of the spindle microtubules in cross-section, the tilt data was recorded and tilts were rectified during model building. Micrographs were taken at an approximate magnification of 21,000 on the microscope, and true magnification was calibrated using a carbon replica grating of known spacing.

3D Reconstruction and Modeling

Microtubule tracking and modeling were as previously described (McDonald et al., 1991, 1992; Ding et al., 1993). Briefly, the operations are as follows: EM negatives of spindle cross-sections are placed on a light box and relevant portions are digitized with a Dage 81 MTI video camera connected to a Parallax 1280 graphics device in a Microvax III computer. Images of successive sections were aligned, and an operator tracked individual microtubules from beginning to end by placing a model point in the centers of each microtubule cross section. Once all the microtubules in every section have been identified, a 3D model is displayed. The correct lengths of the spindle microtubules are calculated after taking into account tilt and section thickness. At this point the distribution of microtubules can be used for various quantitative analyses, including the use of the programs described in McDonald et al. (1991).

Results

Images of Cryofixed and Freeze-substituted Yeast Cells

Fig. 1 shows a longitudinal view of a mitotic spindle in a yeast cell prepared for EM by high pressure freezing and freeze substitution (HPF/FS, see Materials and Methods). Cryofixed and freeze-substituted yeast cells have previ-

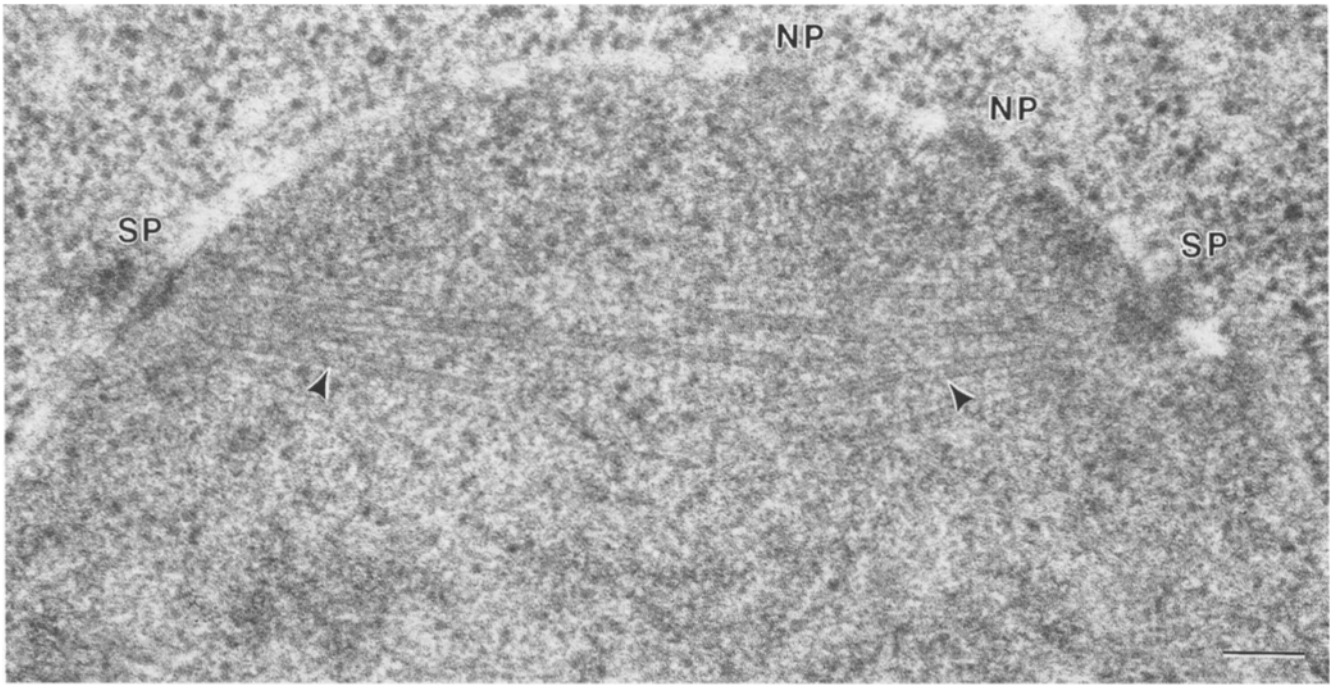

Figure 1. Electron micrograph of a longitudinal section of a yeast spindle in a cell prepared by HPF/FS (see Materials and Methods). The SPBs (*SP*), nuclear pores (*NP*), and microtubules (*carets*) are indicated. Bar, 0.1 μm.

ously been shown to display excellent morphology (Heath and Rethoret, 1982; Tanaka and Kanbe, 1986; Baba et al., 1989; Ding et al., 1993) and have possibly fewer distortions than are seen in cells chemically fixed at room temperature. Indeed, the spindle displayed in Fig. 1 shows microtubules in longitudinal view that are well contrasted, straight, and appear to have uniform thickness along their length in a dense and uniform nucleoplasm. Furthermore, the nuclei in cells at early stages of mitosis, like the one in Fig. 1, appear round and the envelope, spindle pole bodies (SPBs), and pores are all well preserved. The lack of distortion seen in HPF/FS cells gives us confidence that the measurements presented below are accurate. Further differences are seen when cross sectional images of nuclear microtubules from cells prepared by HPF/FS (Fig. 2 *A*) are compared to similar images of cells prepared by chemical fixation (Fig. 2 *B*). Images of microtubule cross sections in HPF/FS prepared cells reveal large lumens surrounded by thin walls in which protofilament structure can be seen. Microtubule cross sections from chemically fixed cells are less regular, and appear smaller and distorted. Overall, we believe that the HPF/FS prepared cells used in this study have suffered less distortion in microtubule and nuclear architecture, and therefore in spindle structure, compared with cells that had been fixed by conventional methods.

Spindle Reconstructions

Fifteen mitotic spindles from *S. cerevisiae* varying in length from 0.6 μm to 9.4 μm have been reconstructed from images of complete serial cross sections. Fig. 3 shows 24 representative cross section images that constitute most of the data set from a 1.48-μm spindle. Microtubule cross sections have been tracked from section to section, and polarity assigned based on the proximity of the microtubule end or ends to an SPB. The criteria for assigning the end of a microtubule to an SPB involves examining each microtubule and its neighbors in the sections that contain the SPB. The SPB is usually seen in two or three sections because it is tilted relative to the spindle axis and it is somewhat curved (Figs. 1 and 3). A microtubule is defined to end "at the pole" if it and some of its neighbors end in the same section, and if the next section past the end of the microtu-

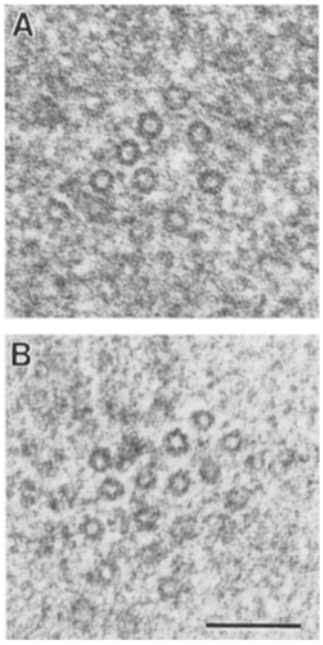

Figure 2. Comparison of microtubule structure in cross sections from cells prepared by HPF/FS (*A*) and chemical fixation (*B*, see Materials and Methods). Bar, 0.1 μm.

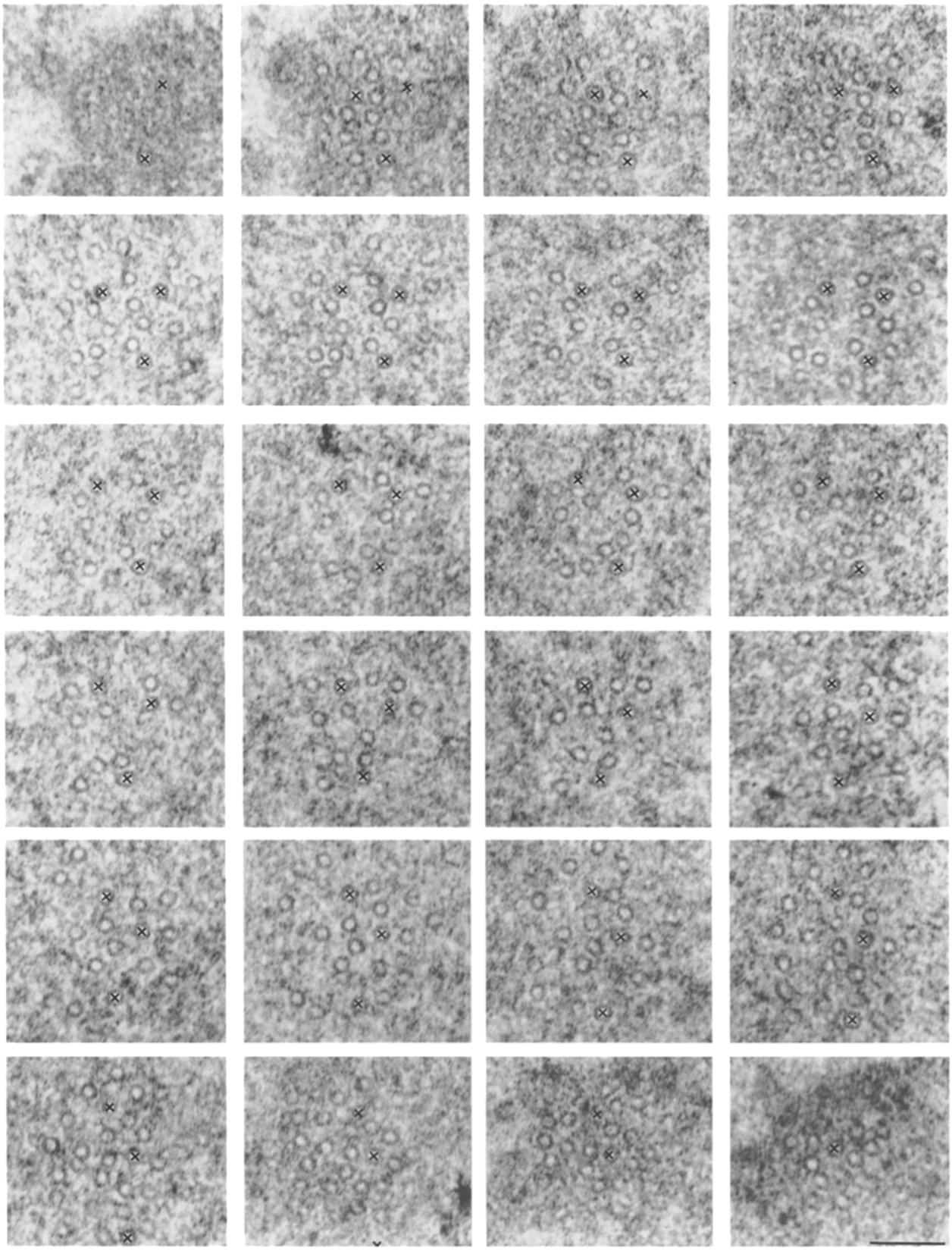

Figure 3. Serial cross sections for a spindle, starting at one pole (*upper left*) and continuing left to right, top to bottom to the other pole. The spindle (No. 9 in Fig. 5; Table I) consists of 36 sections, of which 24 sections are shown here. The sections not shown are distributed throughout the spindle and no gap between the sections displayed is larger than one section. The three continuous microtubules in this spindle are marked with an *x* to aid understanding the nature of microtubule tracking, and of the assignment of polarity. Bar, 0.1 μm.

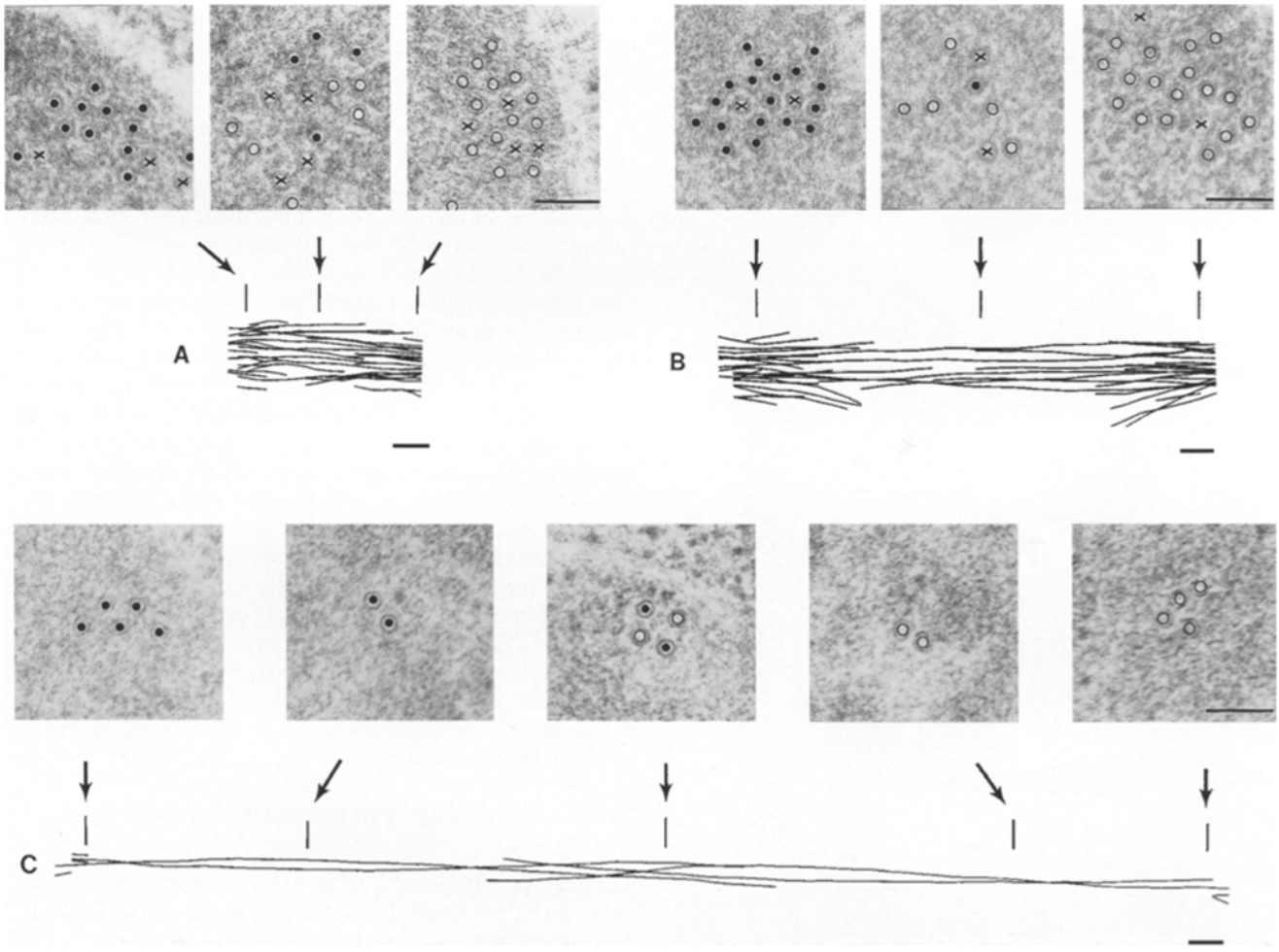

Figure 4. Representative reconstructions of short (*A*, No. 1, Fig. 5; Table I), medial (*B*, No. 7, Fig. 5; Table I), and long (*C*, No. 13, Fig. 6; Table I) mitotic spindles assembled as described in Materials and Methods. Sample cross section micrographs are shown for each reconstruction and the approximate position of each cross section is marked by an arrow and a tick mark. The polarity of the microtubules in each micrograph is indicated by marking the microtubule with a closed circle if it originated from the left pole, an open circle if it tracked to the right pole, and an x if the microtubule was continuous. Bars, 0.1 μm.

bules contains dense SPB material in the vicinity of the microtubule being considered. In the reconstructions presented, all microtubules studied (n = 508) were tracked to one or both SPBs, and fragments of microtubules in the nucleoplasm were not found.

In most cases (94%), one microtubule end is associated with an SPB and the other end is free in the nucleoplasm. We presume that the end of the microtubule defined as associated with an SPB is its minus end. For a minority of microtubules (6%, n = 30), both ends fit the criteria for SPB association. We call these "continuous" microtubules, and we are unable to assign them a polarity. The term "continuous" does not imply that these microtubules have extraordinary structure or that SPBs have the ability to capture a microtubule plus end. We are simply limited in 3D resolution by the 30–50-nm thickness of each section. To illustrate the end assignments of microtubules, the continuous microtubules are identified from one SPB to the other in Fig. 3.

After the microtubules in a spindle have been identified and tracked, a model of the complete spindle can be generated, such as the three shown in Fig. 4. Sample images of cross sections through spindles of various lengths are shown with the polarity of the microtubules indicated. Whereas the reconstructions are useful for visualizing the 3D structure of spindles, comparisons of the organization of spindles can often be better made by using different forms of data presentation, such as two dimensional microtubule overlap diagrams (Figs. 5 and 6). These figures display all the microtubules in each of the 15 spindles reconstructed, where the individual microtubules are arranged by polarity and length. The numbers of microtubules in the 15 reconstructed models are tabulated in Table I. The set of spindles covers the range of spindle lengths (<1.0 μm–~10.0 μm) expected in haploids (Byers and Goetsch, 1975*a*; King et al., 1982). Two reconstructed spindles, (Nos. 13 and 15, Fig. 6; Table I), were derived from a diploid strain used early in the analysis. These two spindles have microtubule numbers and organization similar to what was observed for long spindles (>2.5 μm) from the haploid strain, so we believe that ploidy is not an important factor for microtubule number at this late stage of

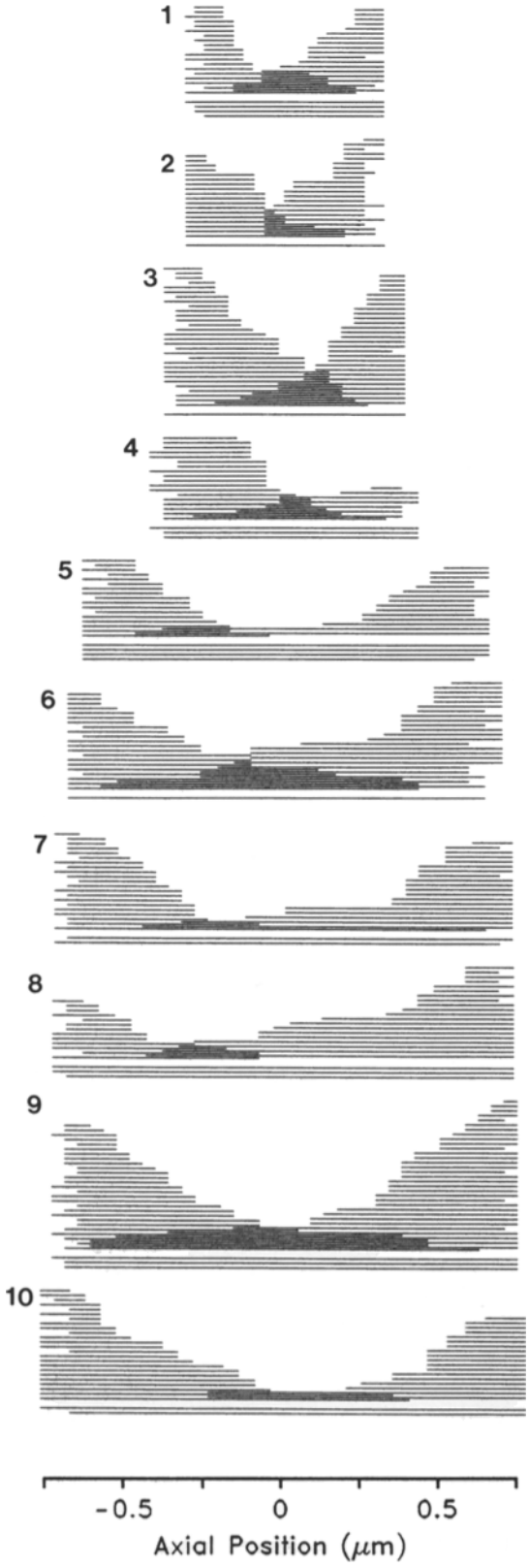

Figure 5. Microtubule overlap displays for the four short (Nos. 1–4) and the six medial spindles (Nos. 6–10). Each line represents a single microtubule, and microtubules from each half spindle are arranged top to bottom according to the position of their plus ends along the spindle axis. The ends at each side of the display are the minus ends. They do not all start from the same section, because the spindle pole body is tilted relative to the spindle axis and/or the plane of section (see Figs. 1 and 3). The continuous microtubules in these reconstructions are displayed under the arrays of microtubules for which polarity was assigned. The numbers of different class microtubules in these reconstructions are tabulated in Table I.

mitosis. These long spindles can lack continuous microtubules, a feature displayed in two spindles of the data set. Finally, the sets of 2–4 long microtubules from each SPB in the long spindles twist around each other, as seen in Fig. 4 *C*. If viewed end-on from the SPB, the twist is left-handed (counter-clockwise) and has a pitch of ~2–2.5 μm.

We were also able to make a few observations about the organization of the cells containing the spindles that were reconstructed. Among these 15 spindles, 11 (Nos. 1–10, Fig. 5; No. 12, Fig. 6; Table I) that ranged in length up to 3.06 μm were found in the mother cell, whereas the remaining four spindles (Nos. 11 and Nos. 13–15, Fig. 6, Table I) ranging from 2.71 μm to 9.41 μm in length were found to extend through the bud neck from the mother into the daughter cell. We observed spindles of ~3.0 μm in length that are entirely in the mother cell. These spindles are longer than the length (<0.9 μm) reported by Byers and Goetsch (1975*a*). We confirm the observation by Byers and Goetsch (1975*a*) that the nuclear envelope is collapsed around the center of the spindle at later points in mitosis. Constriction of the nuclear envelope was seen in all the spindles that extended through the bud neck, but can extend past the limits of the bud neck. This constriction was observed over a long distance in reconstruction No. 15 (Fig. 6), where the cross section of the nuclear envelope showed just enough space in the nucleus to accommodate the spindle microtubules (i.e., Fig. 12 *D*).

Spindle Microtubule Numbers, Length, Distribution, and Packing

The reconstructions of mitotic spindles contained a maximum of 62 microtubules and a minimum of 8 (Table I). The short spindles (Nos. 1–4, 0.63–0.86 μm in length, Fig. 5; Table I) contained an average of 42 (±12) microtubules that were equally distributed between the two SPBs (avg. 21 ± 7). All of the short spindles contained continuous microtubules, and most of them included enough microtubules from each SPB to have one end on each of 16 kinetochores. One short spindle (No. 4, Fig. 5; Table I) is quite asymmetric, with only seven microtubules on one SPB. Such asymmetry may indicate difficulties in identifying all the microtubules in this spindle, or it may represent a bona fide spindle structure resulting from some level of dynamic behavior. The medial spindles (Nos. 5–10, 1.30–1.55 μm in length, Fig. 5; Table I) contain approximately the same number of microtubules (avg. 44 ± 8) as the short spindles, even though the spindles themselves are longer. Microtubule number begins to fall with spindles Nos. 11 and 12 (Fig. 6; Table I), coincident with the first observation of spindles passing through the bud neck. Further reduction in microtubule numbers is observed in the longest spindles (Nos. 13–15, Fig. 6; Table I), all of which extend through the bud neck. The average number of microtubules in the five long spindles (Nos. 11–15, Fig. 6; Table I) is 15 (±7).

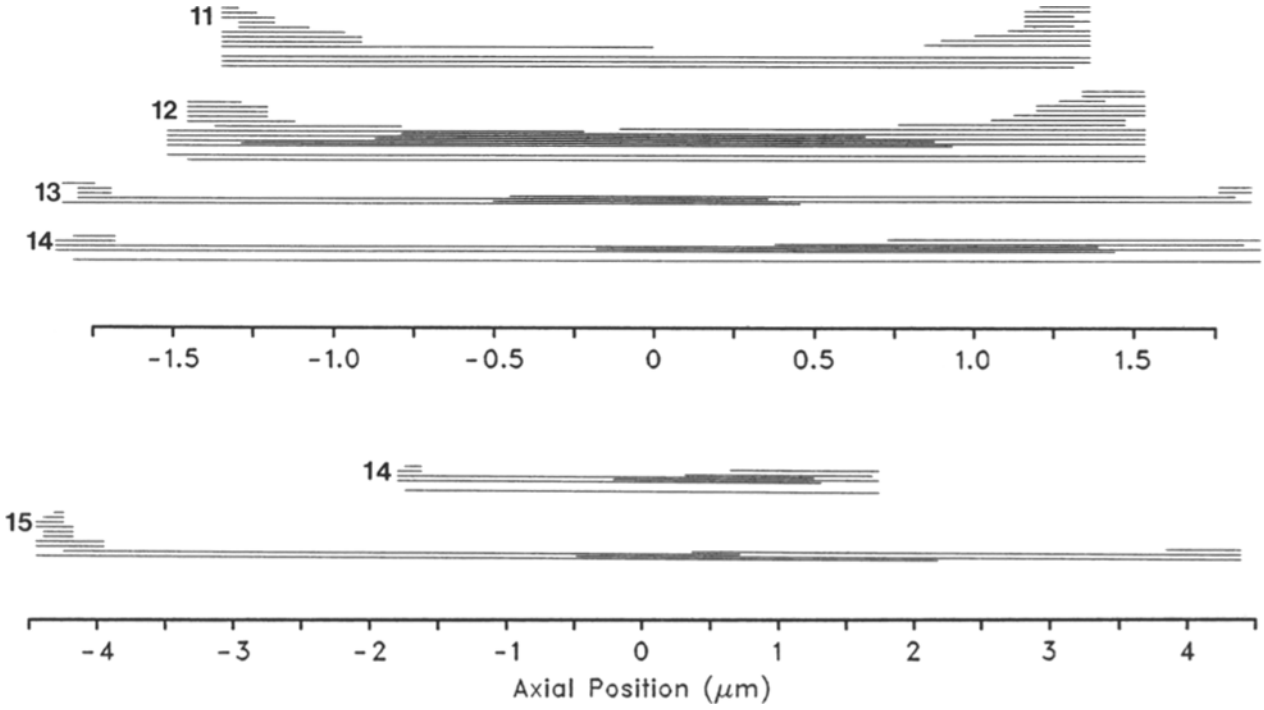

Figure 6. Microtubule overlap displays for the five long spindles (Nos. 11–15) are as in Fig. 5, but plotted on two different scales to accommodate spindle number 15. Spindle 14 is plotted on both scales to show relative size. The top set of spindles (Nos. 11–14) are on the same scale as Fig. 5, and data from all these spindles are included in Table I.

This trend of decreasing microtubule number with increasing spindle length is shown graphically in Fig. 7 *A*. Finally, Fig. 7 *B* shows that the mean length of spindle microtubules increases with spindle length. This is expected because microtubule length is limited by spindle length, and in long spindles, some microtubules must be long enough to span at least half of the spindle.

In addition to the attributes of individual microtubules, quantitative analysis was performed to determine the nature of packing of spindle microtubules in cross section using the algorithms of McDonald et al. (1992). A neighbor density analysis (NDA) was used to calculate the density at which microtubules are found at a given distance from one another, which can be used to identify the preferred distance between microtubules if one exists. Fig. 8 shows the results of the NDA for microtubules in the midzone of the short spindles (Fig. 8, *A–C*) and long spindles (Fig. 8, *D–F*). An NDA of all the microtubules in the short spindles shows a weak peak ~45 nm (Fig. 8 *A*). The NDA results were similar for the medial spindles (data not shown). No significant preferred spacing was detected when neighboring microtubules of like polarity in the short spindles were analyzed (parallel, Fig. 8 *B*). However, analysis of the microtubules from opposite poles revealed a preferred spacing of ~45 nm, center-to-center (anti-parallel, Fig. 8 *C*). In the longest spindles, the microtubules at the midzone exhibited a strong tendency to be separated by ~45 nm (Fig. 8 *D*). This preferred spacing was strongest between microtubules of opposite polarity (anti-parallel, Fig. 8 *F*), when compared to the spacing between microtubules of like polarity (parallel, Fig. 8 *E*). These results suggest that increasing spindle length is correlated with close association among anti-parallel microtubules.

Since a preferred distance was detected between anti-parallel microtubules in the spindle midzones of long spindles, these regions were examined in all spindles for higher order organization, such as a particular packing geometry

Table I. Distribution of Microtubules in 15 Spindle Reconstructions

Spindle			Number of microtubules				
Class	Number*	Length	Total	Polar‡	Continuous	Noncore	Core§
		μm					
Short	1	0.63	41	20/17	4	15/14	12
	2	0.63	40	18/21	1	17/21	2
	3	0.77	59	30/28	1	26/28	5
	4	0.86	28	18/7	3	13/4	11
Medial	5	1.30	36	17/15	4	17/12	7
	6	1.38	45	21/23	1	17/20	8
	7	1.46	42	21/19	2	19/15	8
	8	1.47	36	13/20	3	11/17	8
	9	1.48	62	27/32	3	22/26	14
	10	1.55	44	24/18	2	22/17	5
Long	11	2.71‖	21	9/9	3	8/9	4
	12	3.06	24	10/12	2	6/8	10
	13	3.71‖	9	5/4	0	3/2	4
	14	3.76‖	8	4/3	1	2/0	6
	15	9.41‖	13	10/3	0	8/1	4

*The numbering of spindles here is the same as in Figs. 5 and 6.
‡The polar microtubules are shown left/right in Figs. 5 and 6.
§ Core and noncore microtubules are defined in the text, and are the subject of Figs. 9 and 10.
‖Spindles extended through the bud neck.

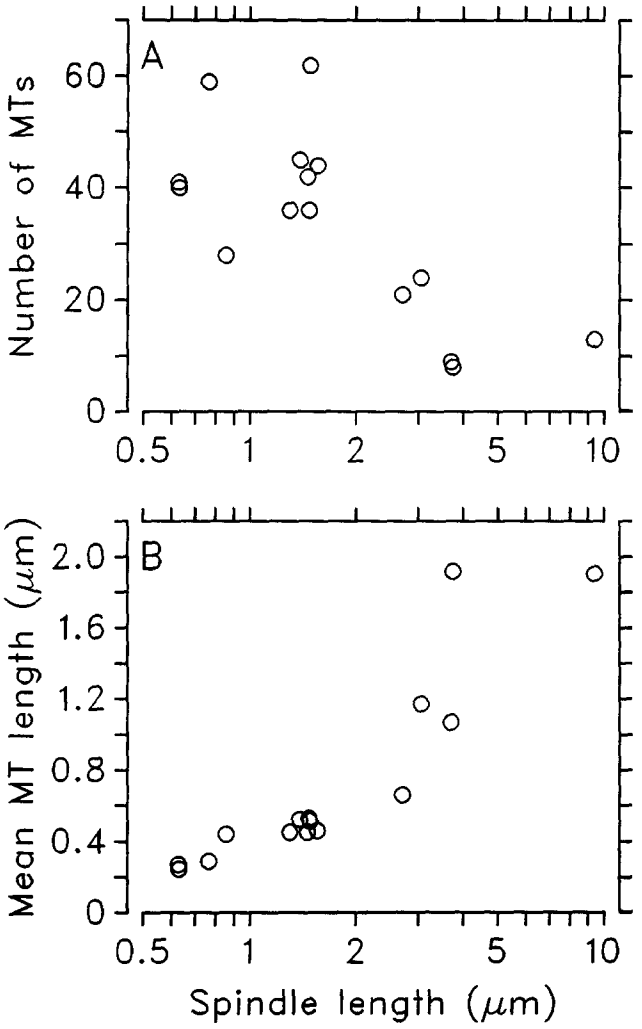

Figure 7. Quantitative analysis of microtubule attributes extracted from the spindle reconstructions, and displayed vs the spindle lengths (x axis, note the logarithmic scale). These attributes include the total number of microtubules in each spindle (*A*), and the mean microtubule length in each spindle (*B*).

as determined by analyzing the angles formed by neighboring microtubules (McDonald et al., 1991, 1992). The cross-sectional structure at the spindle midplanes for short and medial spindles is represented by the examples in Fig. 4, where no consistent packing geometry is apparent and none was found by determining the angular distributions in these spindle midplanes (data not shown). No single example is representative of the structure for longer spindles. Fig. 8 (*G–K*) shows the microtubule arrangement in cross section at the midplane of the 5 long spindles to exhibit the diversity of structure. This diversity includes spindles with and without continuous microtubules. The common theme shown by the three longest spindles (Nos. 13, 14, and 15, Fig. 6) is an array of four microtubules. In two of these spindles (Nos. 13 and 15, Fig. 6), the four microtubules comprise a pair emanating from each SPB. There is no consistent packing geometry for this cluster of four microtubules in the longest spindles. Finally, it may not be a consistent feature of very long spindles (>3.5 μm) that they contain four microtubules, two from each SPB (i.e., Fig. 4 *C*), because a partial reconstruction of an 8.0-μm long spindle only had three microtubules at its midplane (data not shown).

Functional Classes of Microtubules in Mitotic Spindles

One goal of high resolution mapping of microtubules in the yeast spindle was to identify different functional classes of microtubules and to determine their attributes. The two expected functional classes of microtubules were those attached to kinetochores and those that formed an interpolar spindle in association with anaphase B separation of the SPBs. The NDA analysis described above suggested that some anti-parallel microtubules did have a preferred distance of association which could be the result of their involvement in an interpolar spindle. Furthermore, riffling through images of serial spindle cross sections gave the impression that there is a core bundle of microtubules that maintain associations over long distances. The continuous microtubules seemed to be a nucleus for this core, and many of the associations appeared to involve a continuous microtubule and a polar microtubule.

We computed the lengths over which microtubules were "paired" to quantitatively verify the observation of a core bundle of microtubules. Microtubules were defined as paired when they were separated by a distance less than the upper limit of the peak in the NDA graphs (Fig. 8, *A–F*; 45 nm in general, or 55 nm for short spindles). Fig. 9 *A* shows schematically how pairing was computed for two neighbors to a continuous microtubule. The maximum length over which a given microtubule was paired with any of its neighbors was calculated as a single parameter statement that described the extent of pairing for that microtubule. The distribution of maximum pairing lengths for microtubules with nonzero pairing is shown for the short and the medial spindles in Fig. 9, *B* and *C*, respectively. In these histograms, pairing lengths for continuous microtubules are shaded in black. The distribution of pairing lengths for short spindles (Fig. 9 *B*) is unimodal, indicating that core bundle microtubules cannot be reliably distinguished from other microtubules. Conversely, the distribution for medial spindles (Fig. 9 *C*) is bimodal, with one peak due to short pairing distances and a broader peak from longer pairing lengths. This indicates that medial spindles contain two populations of microtubules distinguished by the presence or absence of substantial pairing lengths. The minimal pairing length of 0.24 μm was chosen to distinguish core and noncore microtubules because this value marks the end of the peak of pairing lengths for microtubules not involved in substantial pairings in medial spindles (Fig. 9 *C*), and because all of the continuous microtubules in the short spindles had pairing lengths of at least 0.24 μm. Finally, the reconstructed spindles were reexamined using other pairing lengths to distinguish between core and noncore microtubules. The microtubules involved in core bundles, as defined by these arbitrary pairing distances, were compared with the microtubules identified as being in the core bundle by subjective examination of the reconstruction. The pairing distance of 0.24 μm gave a reasonable correspondence between objective

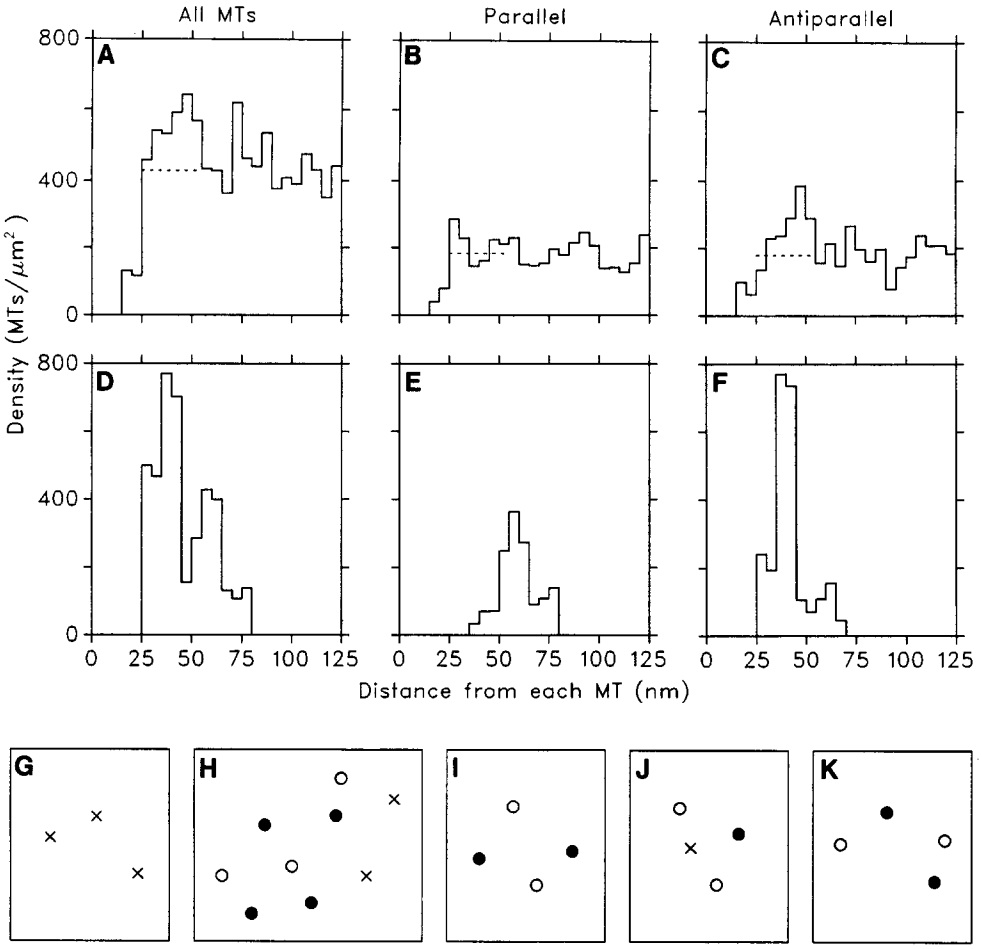

Figure 8. Neighbor density analyses (NDA) for the midplane of short (*A*, *B*, and *C*; spindles Nos. 1–4, Fig. 5, Table I) and the longest (*D*, *E*, and *F*; spindles Nos. 13–15, Fig. 6, Table I) spindles. The average density of neighboring microtubules is plotted as a function of distance from a microtubule. Densities are averaged over 2–5 sections near the midplane of each spindle. The NDA for all microtubules from the spindles are pooled (*A* and *D*), and then categorized by relative orientation with continuous microtubules removed from the analysis (parallel, *B* and *E*; antiparallel, *C* and *F*). The actual midplane packing arrangements (*G*, *H*, *I*, *J*, and *K*) of the five long spindles (Nos. 11–15, Fig. 6, Table I) is shown schematically, where microtubule polarity is defined by the same symbols as in Fig. 4.

and subjective identifications of core bundle microtubules for reconstructions of all lengths.

A medial spindle (No. 7, Fig. 5; Table I) deconstructed into core bundle and noncore bundle microtubules based on the criteria described above is shown in the remaining panels of Fig. 9. The complete reconstruction for this spindle is shown in Fig. 9 *D*, and the core bundle microtubules are displayed in Fig. 9 *E*. This core bundle contains polar microtubule constituents (Fig. 9 *F*; 2 from the left pole, 4 from the right pole) and continuous microtubules (Fig. 9 *G*). Finally, the polar microtubules that are not part of the core bundle are displayed in Fig. 9 *H*.

The importance of continuous microtubules in organizing the core bundle is shown by the fact that two-thirds of the pairing lengths greater than 0.24 μm involved a continuous microtubule, although continuous microtubules are only 6% of the total microtubule population and contribute only 16.6% of the total microtubule polymer in the 15 reconstructed spindles. Of the associations of greater than 0.24 μm in the short and medial spindles, 64% were between a polar and a continuous microtubule, 29% between two polar microtubules, and 7% between two continuous microtubules. Tracking the core bundle of microtubules to the SPB revealed that core bundles extend from the SPB, but are not originated from any given part of the nuclear face of the SPB.

The identification of core bundle microtubules allows a tentative identification of the remaining microtubules as kinetochore microtubules, particularly when viewed in isolation, as in Fig. 9 *H*. Some indication of the behavior of these putative kinetochore microtubules over the course of mitosis can be gleaned from the distributions of their lengths. Fig. 10 shows the length distributions of noncore microtubules (*open bars*) and of core microtubules (*filled bars*) for short (Fig. 10 *A*), medial (Fig. 10 *B*), and 2.7–3.1 μm spindles (Fig. 10 *C*). The mean number of noncore microtubules per spindle is 34.5 for the short spindles and 35.8 for the medial spindles, approximating the 32 expected if one microtubule makes contact with each of the 32 kinetochores. Also, there is no indication that these noncore microtubules shorten in length between the short spindle stage and medial spindle stages. This point is clear from the position of the main peaks in the length distributions (Fig. 10, *A* and *B*), regardless of the identification of core and noncore microtubules. Therefore, both the number and length of the presumptive kinetochore microtubules are nearly the same in short and medial spindles. The number of these microtubules in longer spindles is about half that of the medial spindles. However, the mean length of the remaining noncore microtubules in the long spindles is only somewhat reduced, decreasing from 0.34 μm in the medial spindles to 0.29 μm in the long spindles (Nos. 11 and 12; Fig. 10 *C*). Assuming that these noncore microtubules are kinetochore microtubules, the reduction

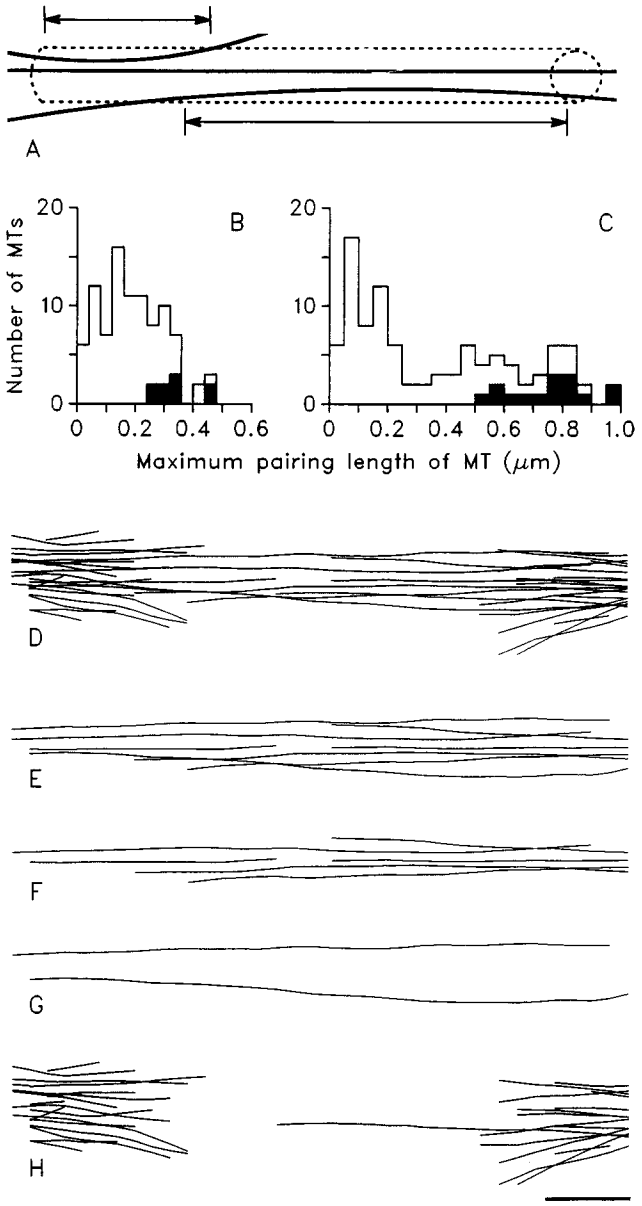

Figure 9. Pairing analysis for identification of core bundle microtubules is shown schematically (*A*). It involves measuring the length over which the distance between two microtubules is no more than 45 nm, center-to-center (*two headed arrows*). Only the segments of microtubules 6 or more sections from the SPB were analyzed to eliminate the effects of general packing of microtubules near the SPBs. The analysis was limited to pairing between antiparallel microtubules and any pairing that involved a continuous microtubule. Microtubules can have more than one pairing partner, but only the longest pairing length has been reported for each microtubule. Pairing lengths of 0–0.45 μm (x axis) are found in the short spindles (*B*; spindles Nos. 1–4, Fig. 5, Table I) and pairing lengths of 0–1.0 μm are found in the medial spindles (*C*; spindles Nos. 5–10, Fig. 5, Table I). The histograms (*B* and *C*) display the number of microtubules (y axes) having a given maximum pairing length (x axes), and the filled regions of the histograms indicate continuous microtubules. Bundling was not examined in the long spindles because the structure is obvious. *D–H* show the deconstruction of a spindle reconstruction (No. 7, Figs. 4 and 5; Table I) into its component parts. By this analysis, the complete reconstruction (*D*) consists of a core bundle of microtubules (*E*) and polar microtubules from each pole (*H*). The core bundle consists of polar microtubules (*F*) and continuous microtubules (*G*). Bar, 0.2 μm.

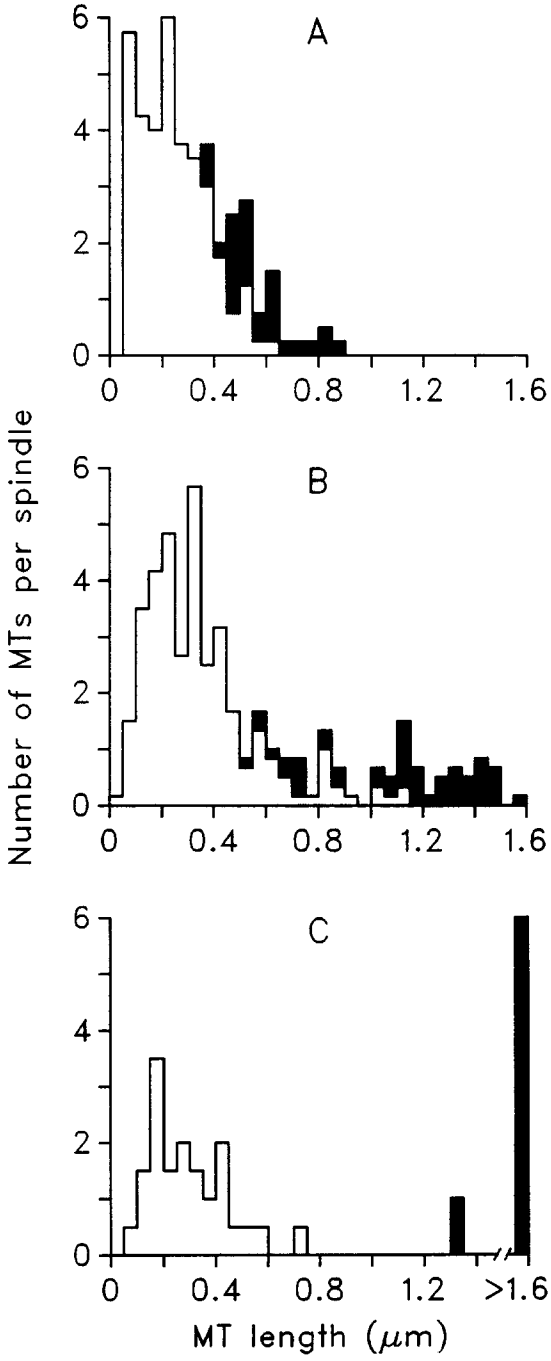

Figure 10. Microtubule length distributions in short (*A*; spindles Nos. 1–4, Fig. 5, Table I), medial (*B*; spindles Nos. 5–10, Fig. 5, Table I), and 2.7–3.1 μm (*C*; spindles Nos. 11 and 12, Fig. 6, Table I) spindles. The number of microtubules (y axis) is plotted vs their lengths in μm (x axis). The numbers of microtubules longer than 1.6 μm has been pooled for the long spindles (*C*). The filled regions of the histograms indicate microtubules identified as core bundle microtubules.

in their numbers and mean length in the longer spindles suggests that anaphase A movements (kinetochore to the pole) do occur.

Based on the supposition that the noncore microtubules are kinetochore microtubules, then the average separation between sister kinetochores can be estimated from the positions of these microtubule plus ends. The distance was measured from the end of each noncore microtubule to the spindle midplane, and this distance was counted as negative for MTs that extended past the midplane. The mean distance was 0.12 μm for short and 0.39 μm for medial spindles, which implies a mean separation between sister kinetochores of 0.23 μm in short and 0.77 μm in medial spindles. As already discussed above, this increase in separation is accomplished by lengthening of the core bundle rather than by any shortening of the kinetochore microtubules. Such lengthening of the core bundle with stable kinetochore microtubule populations should result in an increase in total microtubule polymer in medial spindles as compared to short spindles. Indeed, the increase in spindle length from short to medial is accompanied by an increase in total microtubule polymer from 12.6 ± 3.2 μm (mean ± SD) to 21.7 ± 5.5 μm, respectively.

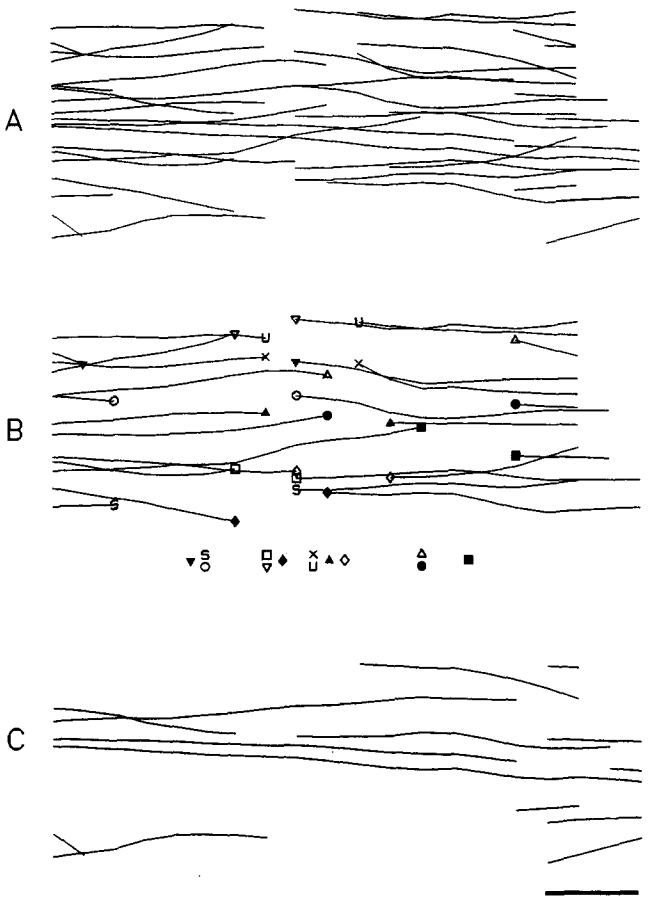

Figure 11. An example of possible end-to-end pairs of noncore microtubules in a short spindle (No. 2, Fig. 5; Table I). The complete spindle reconstruction (*A*) consists of unpaired core bundle and noncore microtubules (*C*) and of paired noncore microtubules (*B*). In this example, pairs were identified using a cone that was 0.25 μm in diameter with a vertex semiangle of 25° extending from the end of one microtubule and choosing the closest end of a microtubule with opposite polarity that lay within the cone. Pairs identified by this technique are identified by like symbols on the ends of two noncore microtubules (*B*), and the same symbols have been placed at the bottom of the panel to indicate the position of the midpoint of the given end pair along the axis of the spindle. The area encompassed by these midpoints has been defined as the midzone. Some microtubule ends appear close, but are not marked as pairs. These ends are separated by significant distances in the dimension perpendicular to the page. Bar, 0.1 μm.

We extensively explored whether the plus ends of opposing noncore microtubules were separated by some characteristic distance. Such an arrangement might be expected if the microtubules were linked to sister chromatids, and may identify metaphase in this yeast. Pairs of opposing microtubules were chosen by a variety of techniques and examined for their geometry, and one example of such pairings appears in Fig. 11 (see legend for details). Unfortunately, no single optimal way to form end-to-end pairs was found. The various criteria used for pair formation greatly affected the identification of individual pairs, the numbers of pairs per spindle, and the average separation between paired microtubule ends. The example of Fig. 11 is, however, quite typical of results from short spindles with rather liberal criteria for forming pairs. The pairs shown illustrate the large range in both the separation between paired ends (0.1–0.25 μm) and the positions of pairs along the axis of the spindle. The end-to-end pairs identified in Fig. 11, and found using other pairing criteria, do not show the uniform spacing between the microtubule ends, or the alignment at the spindle midplane that would be expected for a standard metaphase.

Finally, we extended the analysis of the paired microtubules to characterize the midzone region of *S. cerevisiae* spindles. The midzone is defined as the region of the spindle in which the midpoints of end-to-end pairs of presumptive kinetochore microtubules are found (Fig. 11 *B*). The midpoint positions of paired microtubules and the resulting midzones defined by the midpoints were determined for the three shortest spindles (Nos. 1, 2, and 3; Fig. 5; Table I). These measurements reveal a midzone of 0.36 μm (±0.08 μm), comparable to the midzones of 0.36 μm and 0.42 μm for 2.3 μm and 2.8 μm spindles from *S. pombe* (Ding et al., 1993). These midzones are considerably smaller than the 2.1-μm midzone calculated for a spindle from PtK cells (Mastronarde et al., 1993). However, expressing the size of midzone relative to spindle length suggests that *S. cerevisiae* is quite different. The midzones of the short *S. cerevisiae* spindles examined average 53% the length of the spindle, whereas the *S. pombe* midzones are 16% and 18% of spindle length, and the metaphase PtK midzone is 20% of spindle length. The relatively large spindle midzone region in *S. cerevisiae* spindles, together with our inability to identify end-to-end pairs of noncore bundle microtubules makes it difficult to determine if any of the spindles modeled represent a true metaphase in this organism.

Crossbridge Structures between Spindle Microtubules

Examination of micrographs from every stage revealed the presence of crossbridges between spindle microtu-

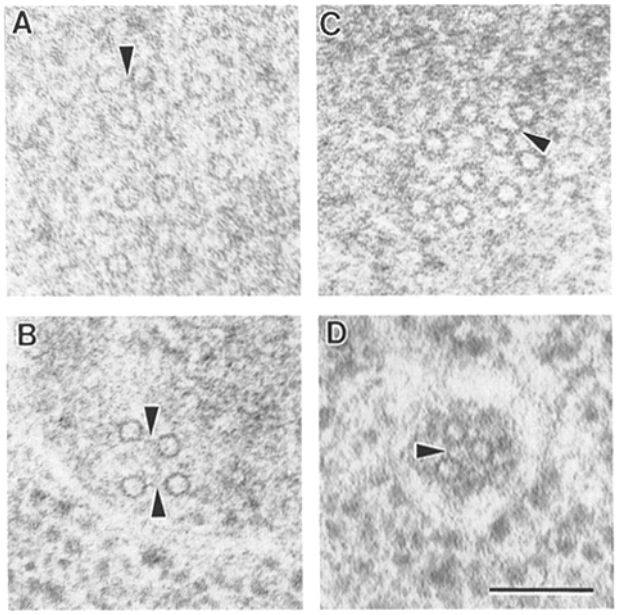

Figure 12. Micrographs displaying crossbridges (*arrowheads*) representative of different spindle lengths (spindle No. 2 [*A*], No. 12 [*B*], No. 13 [*C*], and No. 15 [*D*]; see Table I). All crossbridges displayed connect core bundle microtubules. Bar, 0.1 μm.

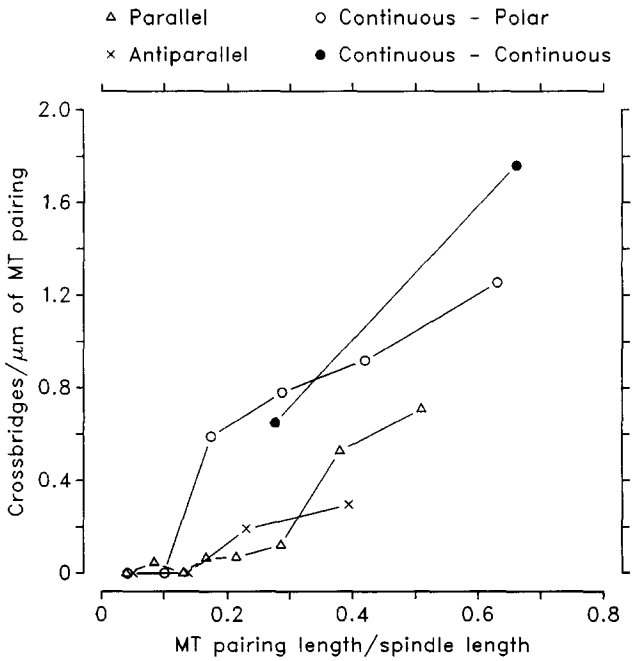

Figure 13. Determination of crossbridge axial density vs relative pairing length as described in Results.

bules. Examples of crossbridges between core bundle microtubules from various cells is shown in Fig. 12. The crossbridges were found between all kinds of microtubules but were predominantly on continuous or long polar microtubules. For example, among the 100 crossbridges found in the 13 spindles with continuous microtubules, 59 were between a polar and a continuous microtubule, and another 17 were between two continuous microtubules, whereas 19 crossbridges were found between parallel polar microtubules, and 5 were between antiparallel polar microtubules. We also noticed that a large fraction of crossbridges were between pairs of microtubules previously identified as being part of a core bundle as described above. In all 15 spindles, 131 crossbridges were identified, of which 85% (n = 111) were between core bundle microtubules, and another 12% (n = 16) were found between core and noncore microtubules. Only four crossbridges (3%) were found between noncore microtubules, and all four were found in short spindles where the core bundle is difficult to identify.

The predominance of crossbridges on continuous and other long microtubules which is correlated with the location of these microtubules in core bundles lead us to ask if the occurrence of crossbridges could be correlated with pairing length between microtubules. For this analysis, we examined the number of crossbridges per unit length of pairing between microtubules. The length over which each possible microtubule pair lay within 42 nm was determined. A maximal distance of 42 nm between paired microtubules was chosen because the center-to-center microtubule separation was <42 nm for 98% of the microtubules bearing crossbridges. The microtubule pairs from the 13 spindles with continuous microtubules were grouped by relative pairing length, which is the actual pairing length divided by spindle length to normalize for spindle length. The crossbridge density was then computed as the total number of crossbridges in the group of paired microtubules divided by the total pairing length (Fig. 13). For all kinds of microtubule pairs, crossbridge density was zero for the shortest pairings and increased progressively with longer pairing lengths. Parallel and antiparallel pairing between polar microtubules had low and comparable crossbridge densities. Pairs of polar and continuous microtubules had much higher crossbridge densities, particularly for the shorter pairing lengths. Among the spindles with continuous microtubules, the highest densities, 1.8 crossbridges/μm, were found for continuous–continuous microtubule pairs with the longest pairing lengths. Only for the longest spindle (No. 15, Fig. 6, Table I) was there a higher density for antiparallel than for parallel pairings (2.9/μm vs 1.9/μm). This analysis reveals that crossbridges are found primarily on core bundle microtubules, and that the density of crossbridges increases with pairing length between microtubules, suggesting that crossbridges may have a role in core bundle formation or stability in these spindles.

Discussion

We have examined the trajectories of spindle microtubules in HPF/FS-prepared samples of wild-type *Saccharomyces cerevisiae* and have obtained information about spindle design at various stages of mitosis. In agreement with previous studies (for review see Byers, 1981*a*), the 3D reconstructions show that spindles of this yeast resemble those from other organisms in that they are formed from two arrays of microtubules, each emanating from its respective SPB. Very short spindles contain enough microtu-

bules to have one microtubule associated with each kinetochore and several to form an interpolar spindle. There is, however, no indication of an ordered metaphase plate. In medial spindles, a core bundle of interpolar microtubules is evident, but there are still enough polar, noncore microtubules to allow one for each kinetochore. The inferred positions of sister kinetochores are more separated in the medial spindles. The transition from a medial to a long spindle occurs at about the time the spindle moves into the bud neck when the pole-to-pole distance is ~3.0 μm. These long spindles contain a core interpolar spindle of 4–10 microtubules, which are apparently sufficient for anaphase B separation of the SPBs (Sullivan and Huffaker, 1992). As the long spindles increase in length, the core bundle microtubules elongate and the number of polar, presumptive kinetochore microtubules decreases. We cannot determine if this decrease in kinetochore microtubule number is the result of uniform shortening and loss of these microtubules, or is the result of individual, stochastic events for each microtubule. Our data are compatible with the idea that an initial phase of spindle elongation promotes sister chromatid separation early in mitosis, and that chromosome to pole motion occurs later. Poleward movement of the chromosomes may be synchronous, with some chromosomes reaching the SPB sooner because they started out closer to the SPB on shorter kinetochore microtubules, or it could be asynchronous, so chromosomes begin to approach the SPB independently of each other. Finally, anaphase B contributes the bulk of chromosome separation in this organism, and would appear to involve microtubule lengthening and sliding at the spindle midplane.

Previous analyses of *S. cerevisiae* spindles have been carried out by viewing entire spindles in thick sections using high-voltage electron microscopy (Peterson and Ris, 1976), and by examining isolated spindles (King et al., 1982). Although limited in various ways, these analyses did detect some of the features of yeast spindles that we report here. Peterson and Ris (1976) reported approximately the same number of microtubules/pole as we have found, and suggested that each kinetochore is contacted by only one microtubule. However, their isolation protocol from swelled spheroplasts may have introduced artifacts, as pointed out by Goh and Kilmartin (1993). Indeed, the Peterson and Ris (1976) study included only spindles up to 2.0 μm, because longer spindles did not survive in their preparations. It has been reported that spindles up to 10 μm are present in intact cells (Byers and Goetsch, 1975*a*; King et al., 1982). The study on isolated spindles by King et al. (1982) did include long spindles and clearly demonstrated that microtubule number decreased in longer spindles, as we have observed. Their models of shorter spindles included ones with an apparent core bundle and short polar microtubules similar to the medial spindles reported here. We did not, however, confirm their finding that the longest spindles contained only one continuous microtubule (King et al., 1982). They did attempt to confirm their observations in preparations of whole cells using longitudinal sections (King et al., 1982), but neither of their approaches yielded high resolution reconstructions of microtubule distributions throughout the spindle. The long spindles reported in this study contained an average of 15 (±7) microtubules in contrast to the single continuous microtubule reported by King et al. (1982).

The present study suggests some features of the mitotic mechanism in yeast that have not been previously detected. One such feature is the transition in the structure during anaphase B that gives rise to the long spindles that extend through the bud neck. *S. cerevisiae* does exhibit increasing organization in the interpolar spindle as it enlongates, a feature common in mitotic spindles (Heath, 1980*a*; Ding et al., 1993). The completely reconstructed spindles contain a core bundle with as few as four microtubules, two from each pole, and a few short polar microtubules. A core bundle of microtubules was also detected in medial spindles by identifying microtubules with relatively long pairing distances. These core bundles may include the microtubules that will make up the core interpolar spindle of the long spindles. The same microtubules were independently identified as members of the core bundle by their high axial density of crossbridges. This distribution of crossbridges has several implications. First, the fact that these structures are far from randomly distributed among microtubules of various kinds and lengths supports the idea that the objects identified as crossbridges are actual linkages between microtubules. Second, the predominance of crossbridges on continuous microtubules supports the idea that these microtubules are an important component of the scaffolding for spindles in anaphase B. Furthermore, the positive correlation of increasing crossbridge density with increasing microtubule length and with increasing pairing length suggests that there may be a functional relationship between crossbridges and the formation of an interpolar spindle. Assuming that yeast spindle microtubules display dynamic instability, like the microtubules of other spindles, these findings suggest that crossbridges may stabilize microtubules in the core bundle. Such stabilization may be required, since it appears that this simple interpolar spindle generates sufficient force for anaphase B in yeast (Sullivan and Huffaker, 1992).

Other newly defined aspects of yeast mitosis involve the onset of anaphase, i.e., sister chromatid separation, and the progression of anaphase from this point. The fact that medial spindles contain populations of polar microtubules that are similar in number and length to those found in the short spindles may indicate that early spindle elongation serves to separate the sister chromatids before anaphase A (movement of the kinetochores to the poles). An unambiguous interpretation of our reconstructed spindles is, however, limited by our inability to define metaphase in this yeast. Its closed mitosis further complicates the issue, because almost all SPB separation in this organism is associated with spindle-like structures, and the short spindles studied here could represent a stage of prometaphase. The problem is compounded by our inability to demonstrate that the polar microtubules are indeed kinetochore fibers, because kinetochores cannot be visualized. However, this is a lesser concern because it is hard to imagine what these polar microtubules are doing if they are not attached to kinetochores. Bipolar attachments of sister chromatids without alignment at the spindle midplane defines metaphase in the fungus, *Neocallimastix* (Heath and Bauchop, 1985). It is possible that *S. cerevisiae* has a similar sort of meta-

phase, but our pairing analysis did not detect this type of bipolar sister chromatid attachment that would have presumably yielded a preferred end-to-end distance for paired microtubules. Nonetheless, kinetochore proteins localize along the length of short spindles in *S. cerevisiae* by immunofluorescent staining, and do not define a metaphase plate (e.g., Goh and Kilmartin, 1993).

It is possible that metaphase in this yeast was not recognized because of fundamental differences in its organization from mammalian cells. Yeast centromeres are small, approximately 125 base pairs (for review see Bloom, 1993), and presumably the kinetochores are also small and may function only to attach each chromatid to a single spindle microtubule, but not to its sister chromatid. If the attachment between sister chromatids is at sites distant from the centromere, perhaps the kinetochores can be attached to each pole even when the gap between the ends of the polar microtubules is relatively large, as in the medial spindles where the gap can be nearly a micrometer. Such organization of the sister chromatids seems possible, since *S. cerevisiae* lacks cytologically discernible chromosome condensation, which may limit such flexibility. Such an arrangement is reminiscent of metaphase in the diatoms *Hantzschia* and *Nitzschia* (Tippit et al., 1980). Finally, we still cannot rule out the possibility that metaphase in yeast is rapid and has simply not been observed.

Another aspect of mitosis in *S. cerevisiae* is the behavior of the polar, presumptive kinetochore microtubules in the long spindles. These microtubules are of approximately constant number and average length in the short and medial spindles, but their numbers decline in the long spindles. The fact that the number of polar microtubules falls in longer spindles while the average length of those remaining is approximately the same as that of the polar microtubules in the short and medial spindles can be explained by either of two models. In one model, the polar microtubules are uniformly depolymerized such that the shortest ones are lost, whereas the longest polar microtubules in short spindles give rise to the observed residual population in longer spindles. The second model suggests that the polar microtubules are depolymerized asynchronously and relatively quickly, such that intermediate length microtubules are not observed. Such behavior would be suggestive of microtubule dynamic instability, and it seems plausible that the loss of the polar microtubules in long spindles results from independent microtubule catastrophes (Mitchison and Kirschner, 1984). In either case, microtubule disassembly could contribute to the poleward movement of the chromosomes if kinetochores are still attached to these microtubules. Formally, such movement of kinetochores to the poles is anaphase A. If this is anaphase A, it occurs late during *S. cerevisiae* mitosis and it may occur asynchronously. Asynchronous anaphase has been described in *Saprolegnia* (Heath, 1980*b*) and *Neocallimastix* (Heath and Bauchop, 1985), though in both organisms the onset of chromosome movement begins from a stage that looks like true metaphase. The role of a late anaphase A in *S. cerevisiae* is not clear, but it may be necessary to draw the centromeres close to the SPB to establish interphase nuclear organization or to prevent chromosome breakage during karyokinesis.

Mitosis in *S. cerevisiae* differs in several ways from the comparable process in mammalian cells, where metaphase alignment of chromosomes is clearly defined and is succeeded by anaphase A and then anaphase B. The spindle of this budding yeast is not greatly different from that seen in other fungi (for review see Heath, 1980*a*). Detailed structural studies of mitosis in several fungi have failed to reveal a true metaphase, and Heath (1980*a*) has pointed out that this feature of chromosome behavior may be dispensable for small spindles. Mitosis in the fission yeast *Schizosaccharomyces pombe* does include a metaphase alignment of chromosomes (Uzawa and Yanagida, 1992), but in this organism part of anaphase B precedes anaphase A (Ding et al., 1993).

Interpretation of the reconstructions of *S. cerevisiae* mitotic spindles is limited by several factors. Microtubule dynamics are not known for yeast spindles; if each kinetochore captures one microtubule and the core bundle microtubules are stabilized by crossbridges, it is possible that there is little dynamic behavior. Also, we have not seen kinetochore structures, so correlations of spindle structures with the stages of mitosis (as defined by chromosome movements) cannot be rigorously accomplished, as demonstrated by our inability to define metaphase. Future studies, combining immunoelectron microscopic identification of kinetochores combined with 3D modeling as presented here, will be critical in refining these correlations. Until then, we anticipate that this description of wild-type *S. cerevisiae* mitotic spindles will be useful in the analysis of the localization of spindle components, and of mutants that arrest mitosis or cause aberrant spindle structure.

We are indebted to Andrew Staehelin for use of the Balzers HPF instrument, and would like to thank Mary Morphew for sample preparation, and Mark Ladinsky for supplying serial sections. Lorraine Pillus and Amy Schutz served as critical readers of the manuscript, and their efforts are greatly appreciated. We appreciate the encouragement of several members of the community of yeast cell biologists and important comments concerning mitosis in several lower eukaryotes from Brent Heath.

The Boulder Lab for 3D Fine Structure is supported by a grant from National Institutes of Health (RR00592 to J. R. McIntosh who is a Research Professor of the American Cancer Society).

This work has also been supported by a National Science Foundation grant (to M. Winey, MCB-9357033), and by the Pew Scholars Program in the Biomedical Sciences (to M. Winey, P0020SC).

Received for publication 17 November 1994 and in revised form 7 March 1995.

References

Baba, M., N. Baba, Y. Ohsumi, K. Kanaya, and M. Osumi. 1989. Three-dimensional analysis of morphogenesis induced by mating pheromone α factor in *Saccharomyces cerevisiae*. *J. Cell Sci.* 94:207–216.

Bloom, K. 1993. The centromere frontier: kinetochore components, microtubule-based motility, and the CEN-value paradox. *Cell.* 73:621–624.

Byers, B. 1981*a*. Cytology of the Yeast Life Cycle. *In* Molecular Biology of the Yeast *Saccharomyces*. I. Life Cycle and Inheritance. J. N. Strathern, E. W. Jones, and J. R. Broach, editors. Cold Spring Harbor Laboratory, Cold Spring Harbor, NY. 59–96.

Byers, B. 1981*b*. Multiple roles of the spindle pole bodies in the life cycle of *Saccharomyces cerevisiae*. *In* Molecular Genetics in Yeast. Alfred Benzon Symposia 16. D. von Wettstein, A. Stenderup, M. Kielland-Brandt, and J. Friis, editors. Munksgaard, Copenhagen. 119–133.

Byers, B., and L. Goetsch. 1974. Duplication of spindle plaques and integration of the yeast cell cycle. *Cold Spring Harbor Symp. Quant. Biol.* 38:123–131.

Byers, B., and L. Goetsch. 1975*a*. Behavior of spindles and spindle plaques in the cell cycle and conjugation of *Saccharomyces cerevisiae*. *J. Bacteriol.* 124: 511–523.

Byers, B., and L. Goetsch. 1975*b*. Electron microscopic observations on the meiotic karyotype of diploid and tetraploid *Saccharomyces cerevisiae*. *Proc. Natl. Acad. Sci. USA.* 72:5056–5060.

Byers, B., and L. Goetsch. 1991. Preparation of yeast cells for thin-section electron microscopy. *Methods. Enzymol.* 194:602–608.
Dahl, R., and A. Staehelin. 1989. High-pressure freezing for the preservation of biological structure: theory and practice. *J. Electron Microsc. Tech.* 13:165–174.
Ding, B., R. Turgeon, and M. V. Parthasarathy. 1991. Routine cryofixation of plant tissues by propane jet freezing for freeze substitution. *J. Electron Microsc. Technique.* 19:107–117.
Ding, R., K. L. McDonald, and J. R. McIntosh. 1993. Three-dimensional reconstruction and analysis of mitotic spindles from the yeast, *Schizosaccharomyces pombe. J. Cell Biol.* 120:141–151.
Goh, P.-Y., and J. V. Kilmartin. 1993. *NDC10* (*CBF2*): a gene involved in chromosome segregation in *Saccharomyces cerevisiae. J. Cell Biol.* 121:503–512.
Heath, I. B. 1980*a*. Variant mitosis in lower eucaryotes: indicators of the evolution of mitosis? *Int. Rev. Cytol.* 64:1–80.
Heath, I. B. 1980*b*. Behavior of kinetochores during mitosis in the fungus *Saprolegnia ferax. J. Cell Biol.* 84:531–546.
Heath, I. B., and K. Rethoret. 1982. Mitosis in the fungus *Zygorhynchus moelleri*: evidence for stage specific enhancement of microtubule preservation by freeze substitution. *Eur. J. Cell Biol.* 28:180–189.
Heath, I. B., and T. Bauchop. 1985. Mitosis and the phylogeny of the genus *Neocallimastix. Can. J. Bot.* 63:1595–1604.
Kilmartin, J. V., and A. E. M. Adams. 1984. Structural rearrangements of tubulin and actin during the cell cycle of the yeast *Saccharomyces. J. Cell Biol.* 98: 922–933.
King, S. M., J. S. Hymans, and L. Luba. 1982. Absence of microtubule sliding and an analysis of spindle formation and elongation in isolated mitotic spindles from the yeast *Saccharomyces cerevisiae. J. Cell Biol.* 94:341–349.
Mastronarde, D. N., K. L. McDonald, R. Ding, and J. R. McIntosh. 1993. Interpolar spindle microtubules in PTK cells. *J. Cell Biol.* 123:1475–1489.
McDonald, K. L., E. O'Toole, D. N. Mastronarde, and J. R. McIntosh. 1992. Kinetochore microtubules in PTK cells. *J. Cell Biol.* 118:369–383.
McDonald, K. L., D. N. Mastronarde, E. O'Toole, R. Ding, and J. R. McIntosh. 1991. Computer-based tools for morphometric analysis of mitotic spindles and other microtubule systems. *EMSA Bulletin.* 21:47–53.
Mitchison, T., and M. Kirschner. 1984. Dynamic instability of microtubule growth. *Nature (Lond.).* 312:237–242.
Peterson, J. B., and H. Ris. 1976. Electron microscopic study of the spindle and chromosome movement in the yeast, *Saccharomyces cerevisiae. J. Cell Biol.* 22:219–242.
Sherman, F. 1991. Getting started with yeast. *Methods. Enzymol.* 194:3–21.
Sullivan, D. S., and T. C. Huffaker. 1992. Astral microtubules are not required for anaphase B in *Saccharomyces cerevisiae. J. Cell Biol.* 119:379–388.
Tanaka, K., and T. Kanbe. 1986. Mitosis in the fission yeast *Schizosaccharomyces pombe* as revealed by freeze substitution electron microscopy. *J. Cell Sci.* 80:253–268.
Tippit, D. H., J. D. Pickett-Heaps, and R. Leslie. 1980. Cell division in two large pennate diatoms, *Hantzschia* and *Nitzschia. J. Cell Biol.* 86:402–416.
Uzawa, S., and M. Yanagida. 1992. Visualization of centromeric and nucleolar DNA in fission yeast by fluorescence in situ hybridization. *J. Cell Sci.* 101: 267–275.